SLAC-PUB-3347
May 1984
(T/E/I)

# ASP, A NEW PEP EXPERIMENT TO MEASURE SINGLE PHOTONS*

R. HOLLEBEEK
*Stanford Linear Accelerator Center*
*Stanford University, Stanford, California 94305*

## Summary

The design and construction of a new experiment for PEP designed to measure the flux of low energy photons unaccompanied by any additional photons, or charged tracks will be described. The device consists of arrays of extruded lead glass bars and PWC's in the central region with lead-scintillator shower counters, drift chambers and PWC's in the forward regions.

## Introduction

In May of 1983 a new experiment was approved for installation in IR-10 at PEP, the purpose of which is to search for final states containing a single photon and missing transverse momentum. The experiment is called ASP, which stands for Anomalous Single Photons and was constructed by a group of physicists from SLAC, MIT and Washington.[1] Installation of a the detector began during the December '83/January '84 shutdown and was continued during short accesses to the IR during the spring cycle. During the month of April the beampipe, masking, one-half of the central calorimeter, and the forward shower counters were in place and the first checkout data was taken. Full operation of the device is expected in the fall of '84.

## Single Photon Sources

In the standard model of weak and electromagnetic interactions, single photon events with missing transverse momentum will be produced by the cross section

$$\sigma(e^+e^- \to \gamma\nu\bar{\nu}) \sim \alpha g_{WS}^4 \left(1 + \frac{N_\nu}{4}\right) \cdot \frac{s}{m_W^4} \quad .$$

This cross section was originally suggested by Ma and Okuda[2] as a means of counting the number of neutrinos and hence placing limits on the numbers of lepton generations. The cross section has a contribution proportional to $N_\nu/4$ due to the neutral weak current (fig. 1(a)) and an additional contribution from the charged current (fig. 1(b)). One advantage of this method of counting lepton families is that the cross section is insensitive to the mass of the associated charged lepton and only requires that the neutrino itself be light.

As pointed out by Ellis and Hagelin[3] and Grassie and Pandita,[4] however, a search for final states containing only a single radiated photon is also sensitive to contributions from the production of pairs of unobserved supersymmetric photons, *i.e.* photinos. The cross section

$$\sigma(e^+e^- \to \gamma\tilde{\gamma}\tilde{\gamma}) \sim \alpha^3 \cdot \frac{s}{m_{\tilde{e}}^4}$$

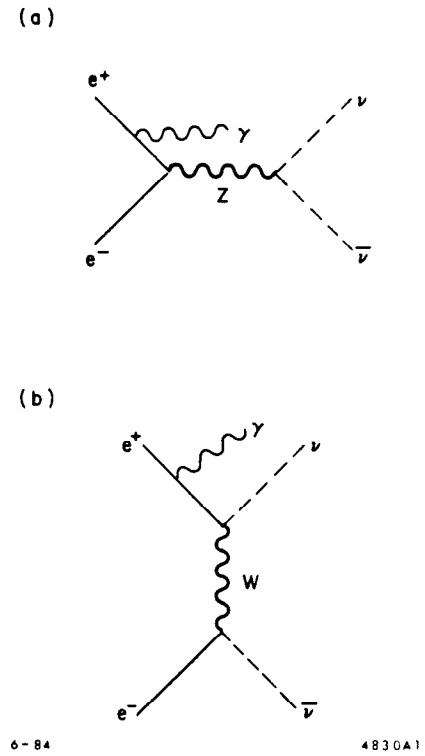


Fig. 1. Single photon contributions from the weak (a) neutral and (b) charged current.

is very similar to the QED cross section for $\gamma\gamma\gamma$ production except for spin factors and the suppression due to $t$-channel exchange of a massive selection *i.e.*, supersymmetric electron.

The differential cross sections for these two processes are also similar, and are given by

$$\frac{d^2\sigma}{dxdy} = K \frac{s}{x(1-y^2)} \left[ (1-x)(1-\frac{x}{2})^2 + \frac{x}{4}(1-x)y^2 \right]$$

where

$$K_{\gamma\nu\bar{\nu}} = \frac{G_F^2\alpha}{6\pi^2} \left[ N_\nu(g_V^2 + g_A^2) + 2(g_V + g_A + 1) \right]$$

and

$$K_{\gamma\tilde{\gamma}\tilde{\gamma}} = \frac{4\alpha^3}{3M_{\tilde{e}}^4}$$

A limit on the total low energy photon flux with missing transverse momentum thus probes the sum of these two sources. The "background" from weak sources is sufficiently small to reach a sensitivity to selectron masses of order $m_{\tilde{e}} \sim 60$ GeV for center-of-mass energies of order 30 GeV. It would, of course, be interesting to try to extend the search for selectrons to

* Work supported by the Department of Energy, contract DE-AC03-76SF00515.

Invited talk presented at the 3rd International Conference on Instrumentation for Colliding Beam Physics, Novosibirsk, U.S.S.R., March 15-21, 1984

masses of order several hundred GeV, since at this point the splitting between $m_e$ and $m_{\tilde{e}}$ indicates a mass scale for supersymmetry breaking which is uncomfortably large.[5]

However, for $m_{\tilde{e}} > \sqrt{2}\, m_{\nu p}$, the weak cross section $\gamma\nu\bar{\nu}$ dominates, and the only way to separate the two contributions is to study the $s$-dependence of the cross section. The weak cross section has an $s$-channel resonance at the mass of the $Z^0$, and there is no $s$-channel process in supersymmetry.

Supersymmetric theories postulate a basic symmetry between boson and fermions in nature. Since to date however, no boson partners to the standard leptons have been found with limits of order 20 GeV for the electron partner,[6] we already know that this symmetry must be badly broken. The details of how this breaking occurs are of course model dependent, but many schemes lead to new particles with masses less than $m_W$. These models are attractive because if the boson fermion mass splittings are not too large,[7] they solve the hierarchy problem within the standard model of weak and electromagnetic interactions.

Despite the obvious successes of the Weinberg-Salam-Glashow model of weak electromagnetism, when looking for new physics, we should also look carefully at its failures. There are of course no obvious experimental failures to date, except that the Higgs boson required for generating masses for leptons and the weak bosons has not been observed. The Higgs boson however has an additional theoretical problem in the standard theory which is that higher order weak corrections to its mass are ultraviolet divergent. This problem is solved in supersymmetry because in the one-loop approximation the relative minus sign between a fermion loop and its boson superpartner causes a cancellation in the contributions to the Higgs mass. This cancellation would be complete if the masses of the fermions and bosons were degenerate but, in general, the correction to the Higgs mass is of the form[8]

$$\delta_{M_H^2} \sim \frac{g^2}{16\pi^2}\,(m_B^2 - m_F^2) \quad .$$

Obviously if the superpartners are too heavy, supersymmetry can no longer be viewed as a solution to the Higgs mass problem.

There are other processes which are accessible to an apparatus with good low energy photon detection. Higher order QED processes like $e^+e^- \to \gamma e^+e^-$ and $e^+e^- \to \gamma\mu^+\mu^-$ provide both a useful calibration for the device and a test of our ability to calculate these processes. In two photon physics, low energy photon detection provides a means of measuring the $\gamma\gamma$ width of the $\eta$ and perhaps even the $\pi^0$. It is also interesting to use the radiative photon tag as a check of our understanding of radiative corrections to other processes such as $e^+e^- \to$ hadrons.

## Apparatus

An end view of the central photon detector for this search is shown in fig. 2. The photons are detected in a five-layer stack of lead glass. Each glass bar is made from $6 \times 6 \times 75$ cm extruded glass of type F2 with 0.35% Ce doping for radiation hardness. Each glass bar is read out by a single XP2212PC phototube (AMPEREX). As shown in fig. 3, the bars are arranged with a staggered pattern along the beam direction

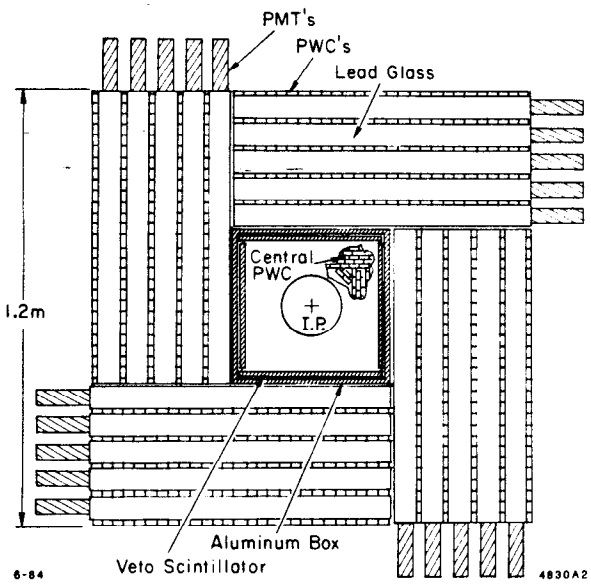


Fig. 2. View along the beam axis of the central photon detector

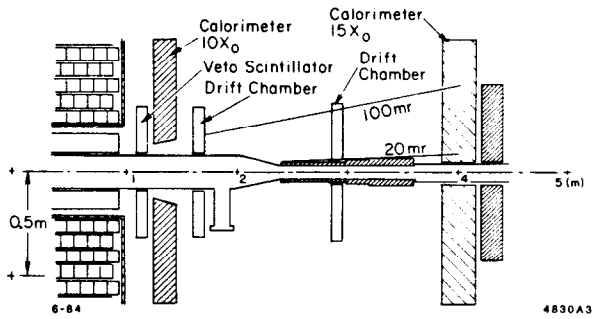


Fig. 3. Side view of the central and forward detectors.

to give optimal resolution in the $z$ coordinate and hence allow separation between photons coming from the origin and those arising from $\pi^0$ photoproduction off the residual gas in the vacuum chamber.

The layers of glass provide five samples of the longitudinal development of the photon shower. There are 632 bars in the total system arranged in four quadrants of 158 bars each. Individual quadrants are complete subassemblies which can be easily dismounted and transported. The two quadrants on the upper and lower left are mounted on rails as are the two quadrants on the right. The entire apparatus splits apart for easy access to the central region.

Each layer of glass is followed by PWC's constructed from aluminum extrusions. The extrusions are eight-cell closed structures with a $1.23 \times 2.36 \times 200$ cm channel and .18 cm wall. The wires are 48 $\mu$ gold-plated tungsten. These extrusions provide the photon pattern recognition in the $xy$ plane.

Inside the calorimeter are two systems, each of which is designed to adequately reject charged particles. The innermost system (central tracker, fig. 4) is made from .9 in $\times$ .4 in $\times$ 88 in aluminum tubes which are thinned to a wall thickness of .012 in by etching. The wire is Stablohm 800 and the tubes are read at each end to give charge division information for the coordinate

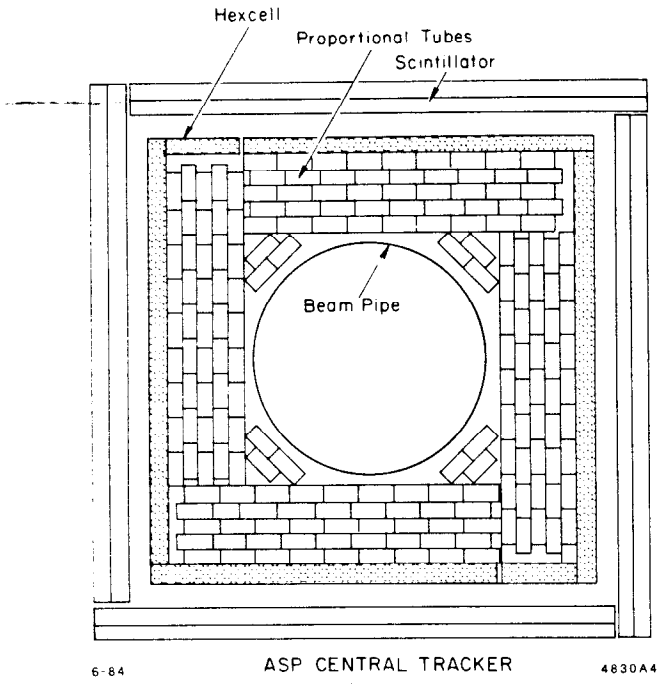


Fig. 4 Central tracker and charged particle veto.

along the wire. The extrusions are glued together in quadrants and mounted on a Hexcell backing material. The tubes are arranged so that radial lines from the origin do not pass through tube walls and extra tubes are added to ensure that a charged particle always passes through at least five layers.

Surrounding the central tracking chamber is a 2 cm thick veto scintillator. Each of the four sides is made from two sheets of 33.5 cm wide $\times$ 225 cm long $\times$ 1 cm Kiowa scintillators. The two sheets could be read independently if necessary, but are presently read at each end by a waveshifter bar and a single phototube. The edges of the scintillators are overlapped so there are no dead regions. Both the central tracking chamber and the veto scintillators split apart when the two halves of the central calorimeter are retracted.

The forward detection systems (fig. 3) are designed to detect the presence of any other particles in an event, to veto low angle QED processes and to measure the energy and angle of electrons from $ee\gamma$ events, thus providing a source of photon events in the central calorimeter. Tungsten masks in the region between 2.5 and 3.5 m are designed to completely shield the central calorimeter from synchrotron radiation and off-energy beam particles lost upstream from the interaction region. Veto scintillators cover the region at the end of the central calorimeter, and two sets of forward calorimeters at 1.5 m and 4 m cover the angular ranges between 20° and 100 mrad and 100 mrad to 20 mrad, respectively. The inside radius of the innermost calorimeter is tapered to eliminate material within the 100 mrad cone.

The details of the forward shower counters are shown in fig. 5. The calorimeters consist of two five-radiation length ($X_0$) modules in the 1.5 meter position and three modules in the 4 meter position. Each module is followed by two planes of offset PWC's arranged to cover the minimum radius of the

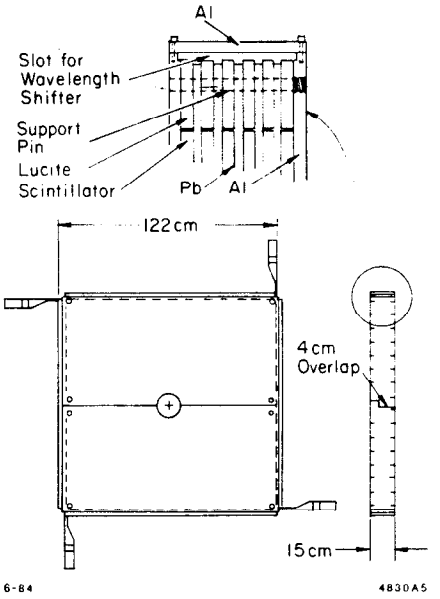


Fig. 5. Forward shower counters.

module as efficiently as possible (fig. 6). The calorimeter modules are lead (0.6 cm Pb + 6% Sb), Polycast PS-10 acrylic scintillator stacks constructed in left and right halves to allow easy assembly around the beam pipe. Each module is readout by four independent phototubes (XP2212PC) viewing waveshifter bars on the four sides of the module. The module halves overlap by 4 cm as shown in fig. 5 to eliminate any inefficiency around the joint between the halves.

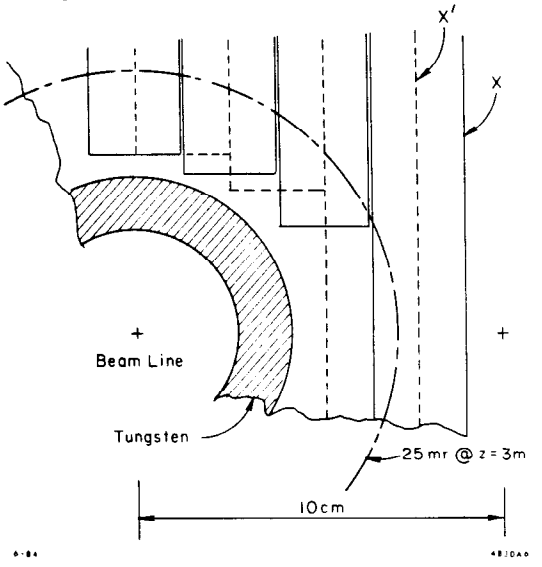


Fig. 6. Forward PWC modules near the beam axis.

At $\sim$ 1.6 m and $\sim$ 2.8 m there are four planes of drift chambers designed to track low angle electrons from $ee\gamma$ events into the rear calorimeter. Measurements of the directions of all three final state particles will allow the reconstruction of a 2 GeV photon in the central resolution with a resolution $\sigma \approx$ 2-3% which is small compared to the resolution of the lead glass. This should provide a useful check on the central calorimeter energy calibration and pattern recognition.

## Backgrounds

Since we want a sensitivity of a few events per 100 pb$^{-1}$, it is important that the backgrounds to the search be well understood and that the apparatus be capable of measuring the characteristics of these backgrounds. The principle technique used to reject backgrounds from QED events is that the transverse momentum of the observed photon must be balanced in $ee\gamma$, $\mu\mu\gamma$, $\gamma\gamma\gamma$ events by the remaining particles. In principle this means that the forward veto system must detect these particles down to angles

$$\theta \sim \frac{p_t^\gamma}{2E_b} \quad .$$

In practice, however, the QED matrix elements are dominated by the case where the $p_t$ is balanced by only one of the remaining particles, yielding

$$\theta \sim \frac{p_t^\gamma}{E_b} \quad .$$

For a 1 GeV photon at 30°, this requires detection down to $\theta \sim$ 35 mrad. Figure 7 shows the results of a QED Monte Carlo calculation of the distribution of $ee\gamma$ events as a function of the $\cos\theta$ of the electron scattered through the maximum $\theta$. Using the forward drift chambers, the apparatus will be able to measure this curve.

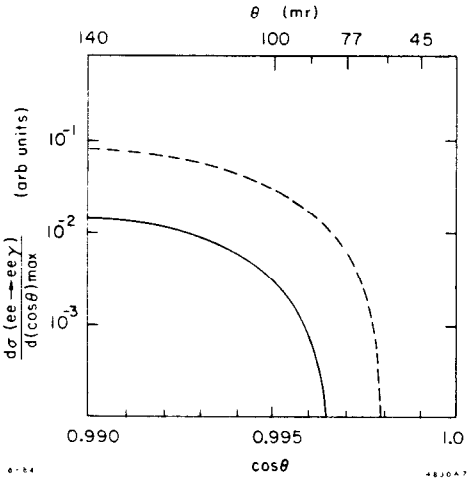


Fig. 7 QED Monte Carlo calculation of $ee\gamma$ versus $\cos\theta_e$.

Additional backgrounds come from $\pi^0$ photoproduction off the residual gas in the vacuum chamber. The number of events which would be observed per 100 pb$^{-1}$ and per centimeter of distance along the beam direction is given by

$$N\ (\mathrm{cm}^{-1}) \approx 4.3 \times 10^{-7} \times p\ (10^{-9}\ \mathrm{Torr}) \times \sigma\ (\mu\mathrm{b})$$

$$\frac{100\ \mathrm{pb}^{-1}}{(\mathcal{L}\ (10^{31}\ \mathrm{cm}^{-2}\ \mathrm{sec}^{-1}))}\ (I\ \mathrm{ma/beam}) \quad .$$

The photoproduction cross section is approximately $10^{-2}\,\mu$ b and requires that the origin of the photon along the beam line be localized to a few centimeters. Additional rejection of these events will come from $\pi^0$–$\gamma$ rejection in the central calorimeter and nuclear fragments in the forward veto system.

## Trigger

The trigger logic for the apparatus is shown in fig. 8. Signals from the phototubes of the central calorimeter are split and sent to a SHAM-BADC system[9] for readout and sums are formed of the energy in eight adjacent lead-glass bars in a layer. Additional sums are formed for the energy in each layer, the energy in a quadrant and the total energy. These sums are sent to gated integrators and the outputs are discriminated and sent to Memory Logic Units, each of which can be used to define several triggers which are patterns of energy deposition in the layers or the quadrants. These Memory Logic Units have twenty inputs which are latched and read via CAMAC. The inputs are then used as address inputs to four 1 k × 4-bit RAM memories which provide forty independent patterns. Twelve of the sixteen outputs from these memories address a second bank of four 4 k × 1-bit memories which contain a zero or a one for trigger definition. The remaining four outputs from the first bank of memories are wired together to form an additional trigger. The trigger pattern in the memories is loaded and checked via CAMAC.

## Prospects

If a selectron exists with a mass of $\sim$ 40 GeV, then a one year run of at least 100 pb$^{-1}$ will yield a sample of $\sim$20 events within 30°. If on the other hand no events are seen in the first 100 pb$^{-1}$, the corresponding 90% C.L. limits on the selectron mass will be $M_{\tilde{e}} > 60$–65 GeV, depending on the backgrounds and the trigger threshold. This limit, of course, depends on the mass of the photino pairs produced with the photon[3] and becomes $M_{\tilde{e}} > 40$ GeV for $M_{\tilde{\gamma}} \sim 10$ GeV. The same run would provide a limit on the number of lepton generations between two and seven in the absence of supersymmetric contributions.


## Acknowledgments

It is a pleasure to acknowledge the efforts of the technical staff for their assistance in the design and construction of the apparatus described in this paper. In particular, we would like to thank K. Sharpaas (engineering), D. Nelson, R.Gray, R. S. Larsen, L. Paffrath (electronics), N. Palmer (vacuum engineering), T. Bell (drafting), and C. Noyer, T. Lyons, R. Baggs, R. Leonard, T. Nakashima, R. Stickley (design and construction).


## References


1. G. Barta, D. Burke, C. Hawkins, R. Hollebeek, M. Jonker, L. Keller, C. Matteuzzi, T. Steele, N. Roe, R. Wilson (SLAC) P. Garbincius (SLAC visitor–Fermilab) A. Johnson, S. Whitaker (MIT) R. Davidson, J. Rothberg, K. Young (Washington).
2. E. Ma and J. Okuda, Phys. Rev. Lett. 41, 289 (1978).
3. J. Ellis and J.Hagelin, Phys. Lett. 122B, 303 (1983).
4. K. Grassie and P. N. Pandita, DO–TH83/25, Dec 1983.

5. In effect for some value of $M_{\tilde{e}}$, the hierarchy problem in supersymmetry is at least as bad as that in the standard theory.

6. L. Gladney, R. Hollebeek, B. LeClaire *et al.*, Phys. Rev. Lett. 51, 2253 (1983). E. Fernandez, W. Ford *et al.*, Phys. Rev. Lett. 52, 22 (1983).

7. S. Dimopoulos, H. Georgi, Nucl. Phys. B193, 150 (1981).

8. J. Ellis, *Nuffield Workshop on the Very Early Universe*, SLAC-PUB-3006.

9. E. Cisneros *et al.*, IEEE Trans. Nucl. Sci. *NS-28*, (1981). M. Breidenbach *et al.*, IEEE Trans. Nucl. Sci. *NS-25* (1978).

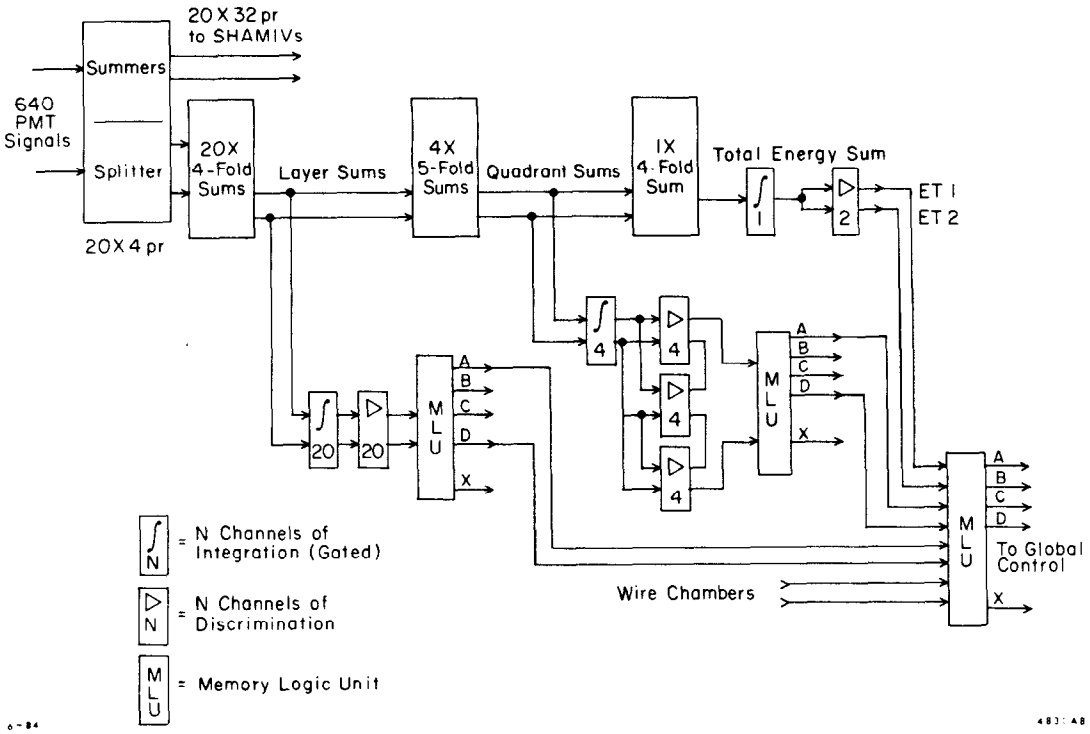


Fig. 8 ASP trigger logic.